An ab Initio and Raman Investigation of Sulfate Ion Hydration

Cory C. Pye* and Wolfram W. Rudolph

Department of Chemistry, Saint Mary's University, Halifax, Nova Scotia, Canada B3H 3C3, and Institute of Virology, Universitätsklinikum Carl Gustav Carus, Technical University of Dresden, Gerichtsstrasse 5, D-01069, Dresden, Germany

Received: September 13, 2000; In Final Form: November 14, 2000

The Raman spectra of ammonium sulfate solution are measured. The geometries, energies, and vibrational frequencies of various isomers of SO_4^{2-} $(H_2O)_n$, $n = 0-6$ are calculated at various levels up to MP2/6-31+G*. These properties are studied as a function of increasing cluster size. The experimental and theoretical vibrational spectra are compared.

1. Introduction

A basic understanding of the solvation properties of ions is essential to understand the properties of electrolyte solutions. For the ubiquitous solvent molecule water, analysis of X-ray and neutron diffraction data clearly demonstrate the concept of hydration shell.[1] This concept, as applied to metal ions, is also supported by Raman spectroscopy and ab initio calculations, in particular, by the authors' work on Li(I),[2−4] Cd(II),[5] Mg(II),[6] Zn(II),[7] Sc(III),[8] Al(III),[9] Ga(III),[10] Be(II), and In(III).[11] Raman studies by one of the authors have focused on sulfato complex formation with Mg(II),[6] Al(III),[12] Zn(II),[13,14] Cd(II),[15,16] and Fe(II).[17] Sulfato complex formation has also been investigated by Rull and co-workers.[18−22] As a prelude to the computational modeling of the vibrational spectra of these ion pairs, we felt that a thorough investigation of the sulfate ion in water was warranted. A search of the literature in the past decade yielded only one ab initio paper.[23] In the work by Cannon, a molecular mechanics model was developed for sulfate in water based on Hartree−Fock (HF/6-31+G*) geometrical and fourth-order Møller−Plesset (MP4) energetic results for the monohydrate. Our work will verify these calculations and extend them, both in the optimization and the frequency calculation up to MP2/6-31+G* levels and by extending the cluster size to contain up to six waters.

2. Materials and Methods

Calculations were performed using Gaussian 92,[24] utilizing the 6-31G*[25] and 6-31+G*[26] basis sets. The MP2 calculations utilize the frozen core approximation. The geometries were optimized using a stepping stone approach, in which the geometries at the levels HF/STO-3G, HF/3-21G, HF/6-31G*, MP2/6-31G*, HF/6-31+G*, and MP2/6-31+G* were sequentially optimized. For the smaller systems, HF and MP2 calculations were also done using the 6-311++G** basis set.[27] Default optimization specifications (rms/maximum displacement smaller than 0.0003/0.00045 au, rms/maximum force smaller than 0.0012/0.0018 au) were normally used. After each level, where possible, a frequency calculation was performed at the same level, and the resulting Hessian was used in the following optimization. Z-matrix coordinates constrained to the appropriate symmetry were used to speed up the optimizations. Since frequency calculations are done at each level, any problems with the Z-matrix coordinates would manifest themselves by giving imaginary frequencies corresponding to modes orthogonal to the spanned Z-matrix space. The Hessian was evaluated at the first geometry (opt = CalcFC) for the first level in a series to aid geometry convergence. For brevity, we refer to 6-31G* as basis set A, 6-31+G* as B, and 6-311++G** as C. Energies were corrected for basis-set superposition error (BSSE) by the standard Boys−Bernardi counterpoise scheme. Details of the spectral measurement in R-format are described in ref 13 and need not be repeated here.

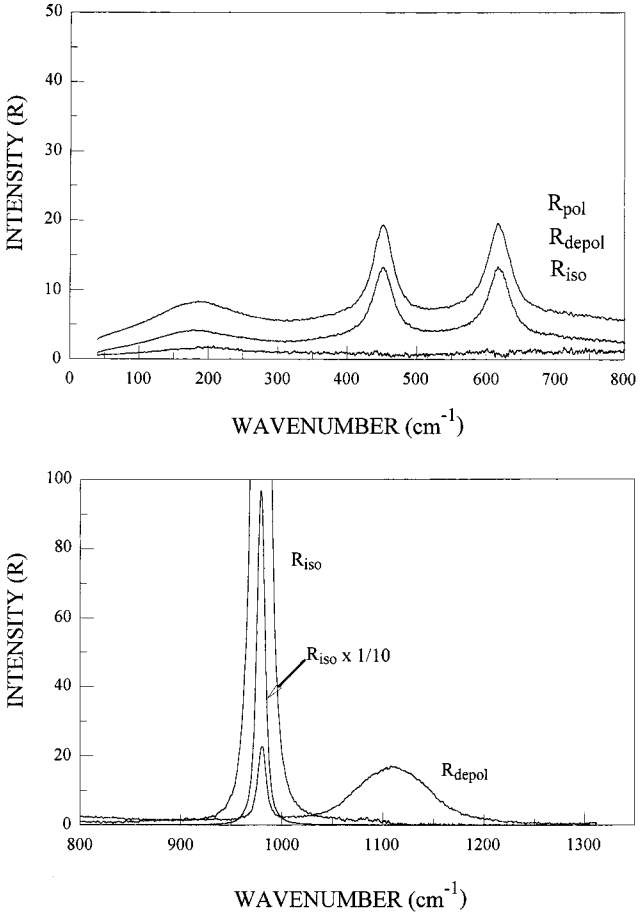

Figure 1. Raman spectra in R-format of a 3.00 mol L^{-1} solution of $(NH_4)_2SO_4$ at 298 K.

10.1021/jp003253n CCC: $20.00
Published on Web 01/13/2001

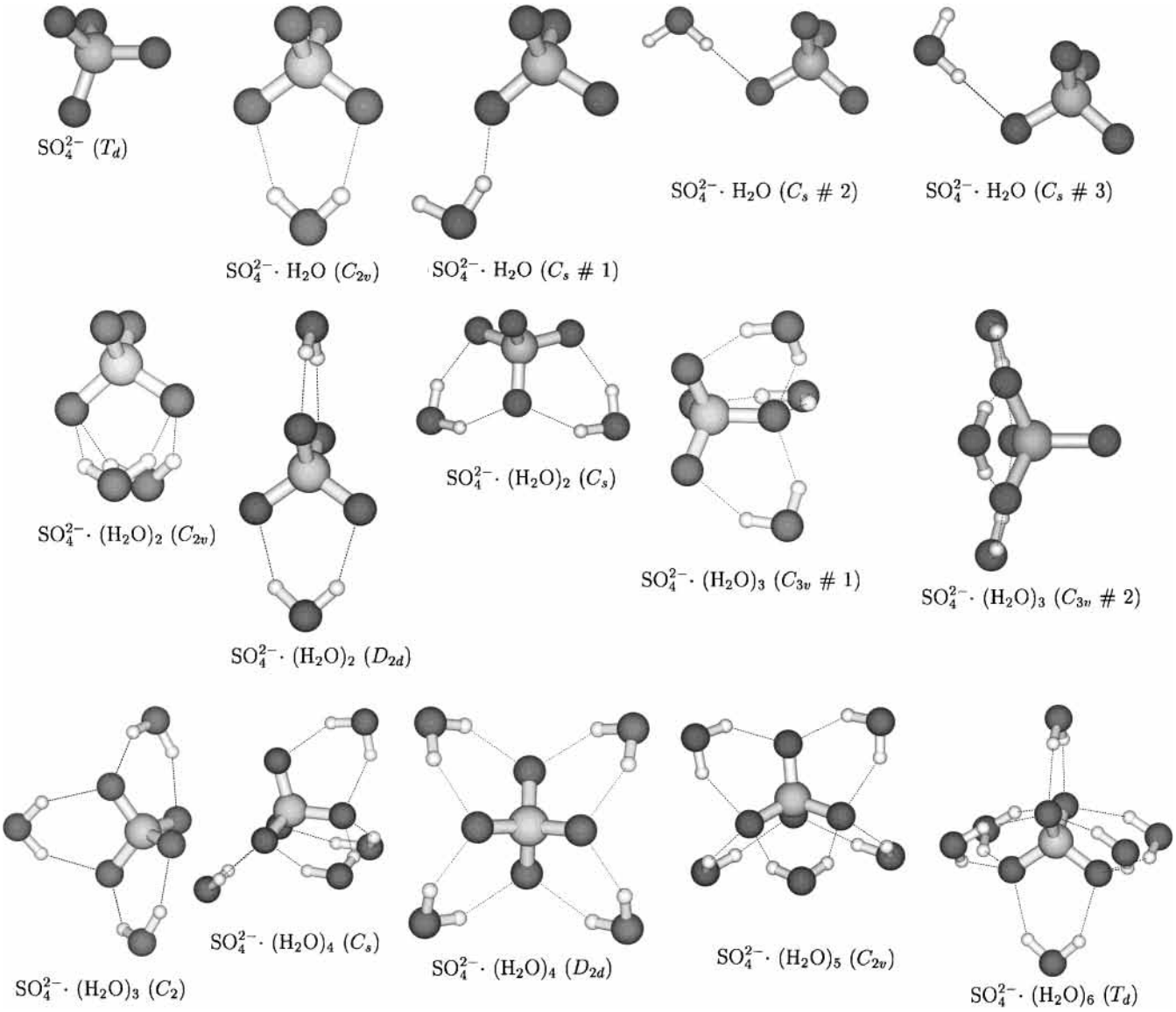

Figure 2. Structures of all species investigated in this study.

3. Results and Discussion

3.1. Experimental Vibrational Spectra of Ammonium Sulfate Solutions. The Raman spectra of aqueous $(NH_4)_2SO_4$ solutions in the concentration range from 0.12 to 3.00 mol L^{-1} were analyzed between 40 and 1350 cm^{-1}. The "free", undistorted SO_4^{2-} ion, of T_d symmetry, has nine modes of internal vibration and spans the vibrational representation $\Gamma_{vib} = A_1 + E + 2T_2$. All modes are Raman active, but only the T modes are IR active. The spectrum of a 3.00 mol L^{-1} $(NH_4)_2SO_4$ solution (see Figure 1) shows the predicted four Raman-active bands for the tetrahedral SO_4^{2-} ion. The $\nu_1(A_1)$-SO_4^{2-} band centered at 981.4 cm^{-1} is totally polarized, whereas $\nu_3(T_2)$-SO_4^{2-}, centered at 1106 cm^{-1}, and the deformation modes $\nu_4(T_2)$-SO_4^{2-} at 617 cm^{-1} and $\nu_2(E)$-SO_4^{2-} at 451 cm^{-1} are depolarized. Table 1 gives the band parameters for the sulfate modes, including the full-width at half-height (fwhh) for all bands. We point out that the fwhh for the bands assigned to degenerate modes are larger than that for the ν_1 mode. For further discussion of these results see refs 13 and 17.

The ν_1-SO_4^{2-} band shape is symmetrical in both polarization arrangements in the concentration range studied and remains so up to 200 °C. However, the band shape was not Lorentzian and thus was fitted with a Gauss−Lorentz profile. At 22 °C, the Gauss−Lorentz factor was 0.735, whereas at 200 °C, it was 0.898, indicating that the band becomes more Lorentzian with increasing temperature. This was also noted in an earlier study within the range 5−80 °C.[28] The position of the peak maximum (± 0.2 cm^{-1}) shifts to lower frequencies with increasing temperature (981.4 at 25 °C, 979.8 at 99 °C, 977.5 at 200 °C for a 3.00 mol L^{-1} solution) and is upshifted with increasing concentration ($980.9 + 0.17\ C_{SO_4^{2-}}$). The fwhh increases with temperature (5.8 at 25 °C, 8.8 at 99 °C, 12 at 200 °C for a 3.00 mol L^{-1} solution) and concentration (3.5 at 0.12 mol L^{-1}, 5.8 at 3.00 mol L^{-1}). The relative molal intensity, S_{981} (SO_4^{2-}), also known as the relative molar scattering coefficient, is 0.778 ± 0.002 and is independent of temperature.

TABLE 1: Band Parameters of Sulfate Modes in 3.00 M Ammonium Sulfate Solution at 298 K

mode	position	fwhh	depol
$\nu_3(T_2)$	1106 ± 2	88 ± 2	0.75
$\nu_1(A_1)$	981.4 ± 0.2	5.8 ± 0.2	0.005 ± 0.002
$\nu_4(T_2)$	617 ± 2	40 ± 2	0.75
$\nu_2(E)$	451 ± 2	34 ± 2	0.75

No sulfato complex formation between ammonium and sulfate is detectable in the spectra. In the low frequency region, only the restricted translation of the water molecules and the water-

TABLE 2: SO_4^{2-} (H_2O) − Electronic Energies of C_s Isomers relative to C_{2v} Structure

	energies (kJ/mol)		
level	#1	#2	#3
HF/A	27.9	28.0	16.2
HF/B	23.1	23.2	13.8
MP2/A	35.1	35.5	19.3
MP2/B	27.2	26.9	14.8

sulfate H-bond stretching mode is detected. Because sulfate forms slightly weaker H-bonds than water, the H-bond stretching mode is observed at slightly lower frequencies.

When polyatomic anions such as sulfate replace water in the first coordination sphere of a cation, marked changes occur in the spectrum of the ligated sulfate, allowing a differentiation between ligated and unligated sulfate. Additionally, for metal cations, a shift or splitting of the metal aqua modes and the appearance of a metal−ligand vibration at low frequencies is often detectable. The study of unligated sulfate in aqueous ammonium sulfate solutions then allows comparison to other sulfate solutions in which ion pairing may be important.

3.2 Ab Initio Calculations: General Description of Structures. *3.2.1. SO_4^{2-}.* The sulfate ion possesses T_d symmetry at all levels investigated. We were initially concerned that some of the valence electrons in this small dianion might not be bound, as manifested by occupied orbital energies greater than the ionization threshold. Our fears were realized for the lower levels (HF/STO-3G, HF/3-21G, HF/6-31G*), but the addition of diffuse functions partially rectified the problem.[29] In addition, the STO-3G and 3-21G basis sets gave larger sulfur−oxygen bond distances than calculations at the other levels. For these reasons, we only report these results for sulfate ion itself. We also calculated the geometry and vibrational frequencies of sulfate at the HF and MP2/6-311++G** level to ascertain any remaining basis set effects.

The geometries and vibrational frequencies of the sulfate ion are given in Table S2 and a structural model is given in Figure 2. The inclusion of correlation effects via MP2 calculations lengthens the S−O bond distance and lowers both the stretching and the deformation frequencies. We emphasize that the high level HF/6-311++G** and MP2/6-311++G** frequencies are within 20 cm^{-1} of the corresponding 6-31+G* frequencies. We also note that, although the 6-31G* basis set usually does well for frequencies as compared to our highest level, the asymmetric stretching mode υ_3 is overestimated.

3.2.2. $SO_4^{2-}\cdot(H_2O)$. A single water molecule may interact with sulfate in one of four ways, as given in Figure 2. One of these coordination models gives rise to a C_{2v} structure containing two hydrogen bonds, whereas the others possess C_s symmetry and a single hydrogen bond. The C_{2v} structure, as expected, affords the lowest energy structure, as shown also by Cannon.[23] In Cannon's work, the S−O−H angle in the C_s structures was constrained to be 180.0, but our structures show considerable deviation from this. Cannon's structures a and b can be identified with our C_{2v} and C_s #2, whereas their structure c corresponds to both C_s #1 and #3 after removing the constraint.

Only the C_{2v} structure gave all real frequencies. All of the C_s structures gave an imaginary frequency whose normal coordinate was of A'' character, corresponding to wagging of the free hydrogen. The difference in zero-point and temperature corrections to the electronic energies is too small to invert the relative electronic energies. The energy ordering of these structures, as given in Table 2, can be rationalized as follows. The most stable configuration is C_{2v}. To bring C_s #3 to the most stable configuration requires only a rotation about the bound hydrogen to oxygen bond of approximately 60 deg, and thus, this configuration is the most stable of the three C_s structures. The other structures require a rotation of 120 or 180 deg and are accordingly higher in energy. In addition, for the first two C_s structures, a second frequency is of very small magnitude (<30 cm^{-1}), clouding the characterization of these species as first or second-order saddle points.

TABLE 3: SO_4^{2-} $(H_2O)_2$ − Electronic Energies of Other Isomers relative to D_{2d} Structure

	energies (kJ/mol)	
level	C_s	C_{2v}
HF/A	1.7	18.1
HF/B	1.9	23.1
MP2/A	1.3	14.2
MP2/B	0.7	18.8

TABLE 4: SO_4^{2-} $(H_2O)_3$ − Electronic Energies of C_{3v} Isomers relative to C_2 Structure

	energies (kJ/mol)	
level	# 1	# 2
HF/A	2.5	0.7
HF/B	2.3	1.0
MP2/A	2.7	0.1
MP2/B	1.5	0.1

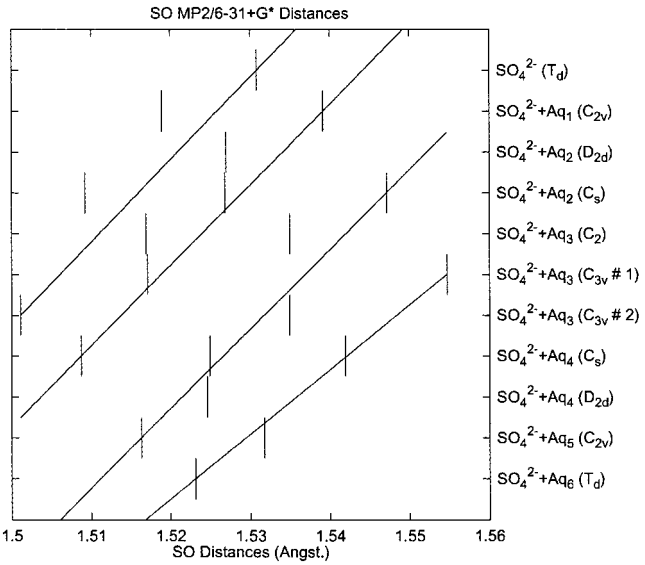

Figure 3. MP2/6-31+G* S−O distance in clusters.

Selected metrical parameters of the C_{2v} complex are given in Table S3. The S−O(free) distance decreases relative to the uncomplexed sulfate, whereas the S−O(bound) distance increases. The hydrogen bonding weakens the S−O bond slightly, allowing the free S−O bond to strengthen. In the same way, the O−H distance increases by about 0.02 Å relative to free water (see Table S4).

The frequencies of the complex are given in Table S5. The water deformation modes increase by about 110−130 cm^{-1}, the water symmetric stretching modes decrease by about 160−270 cm^{-1}, and the water asymmetric stretching modes decrease by about 290−430 cm^{-1}. The changes are more pronounced at the correlated level and are consistent with weakening of the O−H bond. For the C_{2v} complex, the sulfate modes correlate as follows: $A_1 \rightarrow A_1$, $E \rightarrow A_1 + A_2$, and $T_2 \rightarrow A_1 + B_1 + B_2$. The $\upsilon_1(A_1)$ stretching mode is hardly affected by the coordinated water, whereas the $\upsilon_3(T_2)$ stretching mode splits significantly over a range of up to 100 cm^{-1}. The $\upsilon_2(E)$ deformation mode

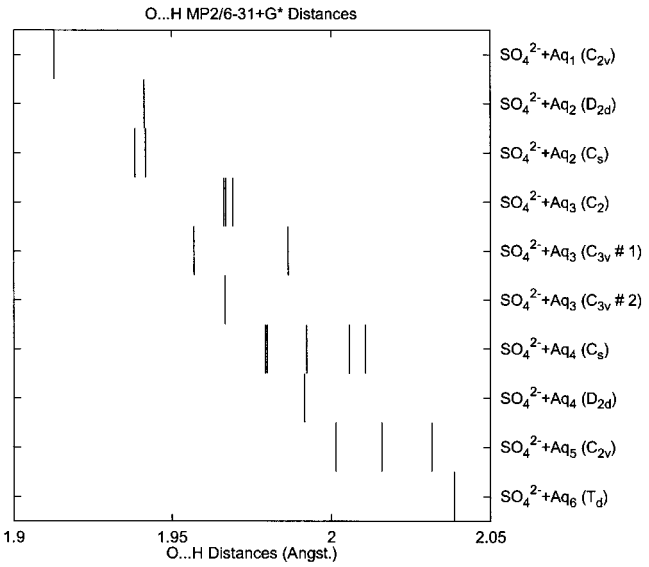

Figure 4. MP2/6-31+G* O···H distance in clusters.

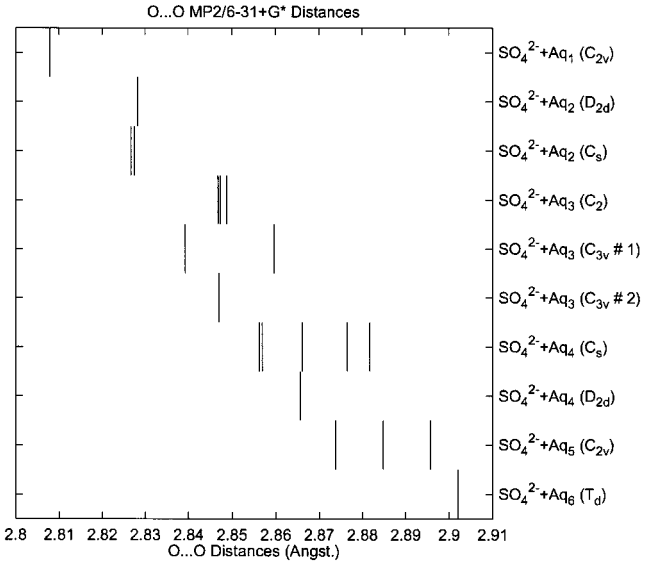

Figure 5. MP2/6-31+G* O···O distance in clusters.

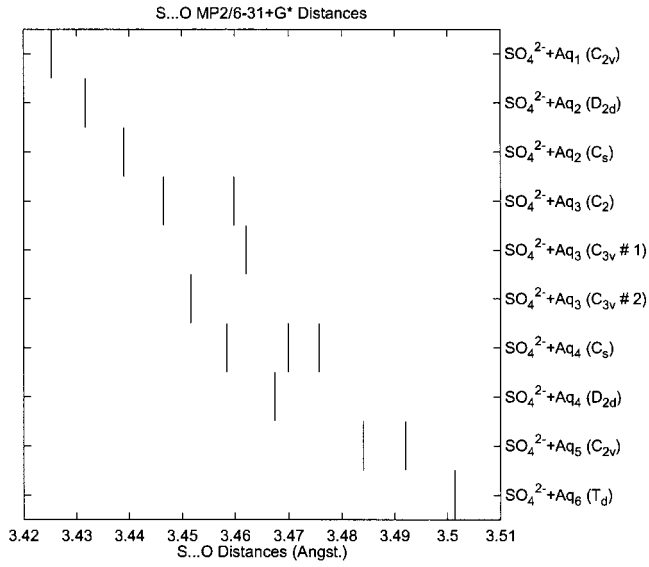

Figure 6. MP2/6-31+G* S···O distance in clusters.

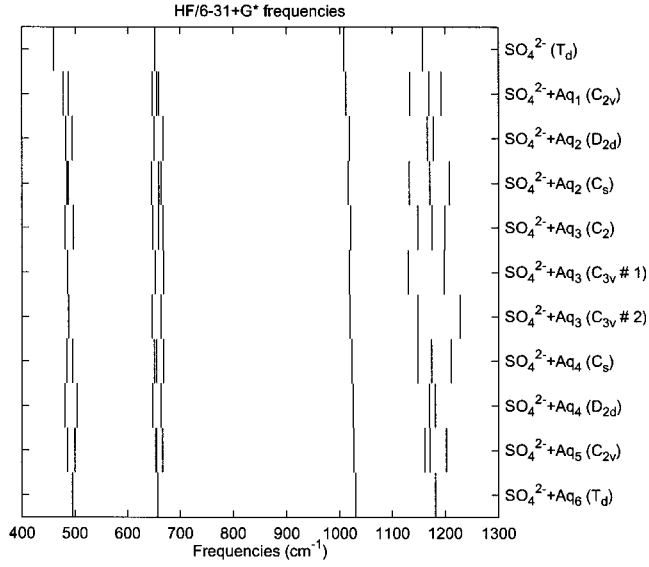

Figure 7. HF/6-31+G* Sulfate mode frequencies in clusters.

splits and is raised in frequency by up to 100 cm^{-1}, whereas the $\nu_4(T_2)$ deformation mode splits by 10−15 cm^{-1} but otherwise does not change.

3.2.3. SO_4^{2-}·$(H_2O)_2$. In the previous section, we have established that water prefers to coordinate to sulfate in a bidentate fashion to form two hydrogen bonds. We may restrict our attention to complexes possessing this coordination mode. For sulfate, there are six such sites available for coordination, corresponding to each pair of oxygen atoms. One possibility is that a site is doubly occupied. In the monohydrate, the mode corresponding to the water translation perpendicular to the water plane is of very low frequency (<100 cm^{-1}), and thus the water may potentially move out of the way to accommodate a second water. We investigated this possibility, which would likely give a C_{2v} structure. If a second water coordinates to the opposite side of the sulfate, so that no sulfate oxygen has more than one hydrogen bond, then this structure possesses D_{2d} symmetry. The only other possibility is that one of the sulfate oxygens has two hydrogen bonds (coordinated to two waters), which would give a C_s structure. We investigated all three structures. The D_{2d} structure is the lowest in energy, followed closely (<2 kJ/mol) by the C_s structure (see Table 3). Differences in zero-point and thermal corrections to the enthalpy amount to less than 0.1 kJ/mol. The C_{2v} structure lies 15−25 kJ/mol higher in energy, and thus it is clear that, although it is a local minimum, it is not thermodynamically favored. Thus we can say that each site prefers only a single water.

The metrical parameters of all three species are given in Table S6. The sulfur−oxygen bond distances across the three isomers are similar and depend (to within ±0.002 Å) only upon the number of hydrogen bonds each oxygen has. Each hydrogen bond lengthens the S−O distance by 0.015−0.020 Å, depending on level. No systematic trends emerged from the OH distance. The hydrogen-bonding indicators (O···H, O···O, S···O) show that the C_s and D_{2d} structures are much more alike than the C_{2v} isomer.

The frequencies of the two important species are given in Tables S7 and S8. As compared to the monohydrated sulfate, the OH stretching frequencies are higher by about 30−100 cm^{-1}, with correlated levels giving a greater change. The bending modes are hardly affected by the additional water. The sulfate modes correspond as follows: for D_{2d}, $A_1 \rightarrow A_1$, $E \rightarrow A_1 + B_1$, $T_2 \rightarrow B_2 + E$; for C_s, $A_1 \rightarrow A'$, $E \rightarrow A' + A''$, $T_2 \rightarrow 2A' + A''$.

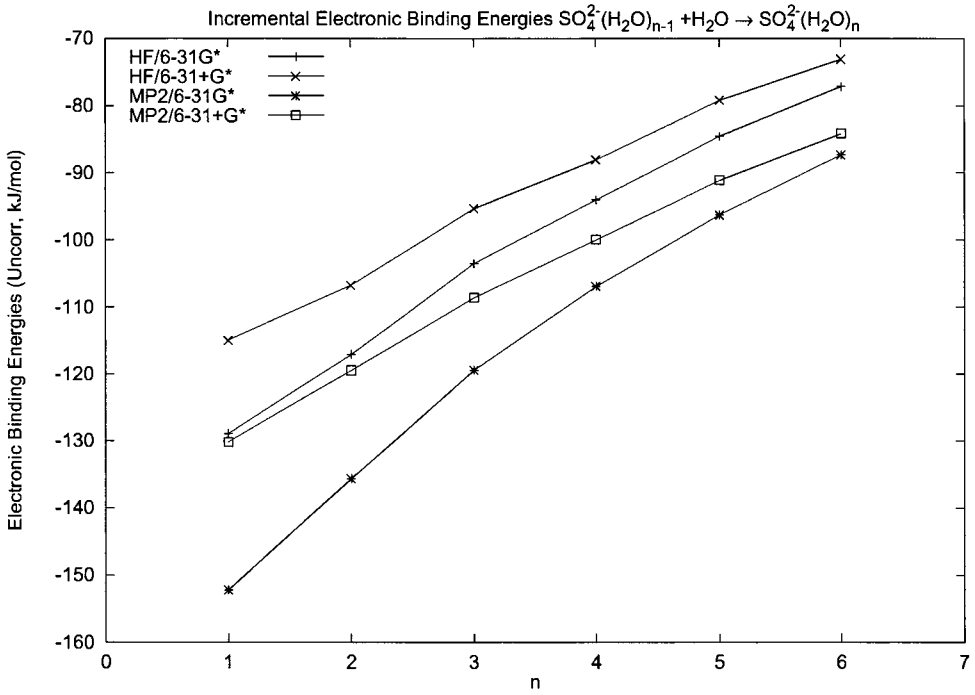

Figure 8. Sulfate incremental binding energies (uncorrected).

As compared to the monohydrate, the modes are slightly increased in frequency.

3.2.4. $SO_4^{2-}\cdot(H_2O)_3$. In the previous section, it was established that sulfate prefers to hydrogen bond to one water per pair of oxygen atoms. If a third water binds to the sulfate, then there are three possibilities. If one of the sulfate oxygens possesses three hydrogen bonds, then the others possess one each (C_{3v} #1). Alternatively, three of the oxygens may possess two hydrogen bonds each (C_{3v} #2, see Figure 2). Finally, two of the oxygens may possess two hydrogen bonds, and the others possess one each, (C_2, see Figure 2). This last structure is electronically the most stable, with the C_{3v} #2 structure within 1.0 kJ/mol and the C_{3v} #1 within 3.0 kJ/mol (see Table 4). The difference in zero-point and thermal energy corrections between the two C_{3v} structures are of the order of 0.3 kJ/mol and between the two most stable structures of around 0.1 kJ/mol and are therefore significant. However, the C_2 structure is stabilized further by these energy corrections.

The metrical parameters of all three species are given in Table S9. The trends are similar as those for the diaqua species. For comparable hydrogen bonds, those in the triaqua are slightly shorter and may indicate some cooperative effects.

The frequencies of all species are given in Tables S10, S11, and S12. The diaqua D_{2d} structure, upon addition of water, can only give rise to the C_2 triaqua structure, whereas the diaqua C_s can give rise to all triaqua species. Therefore, we will make comparisons only with the C_s structure. As compared to the dihydrated sulfate, the OH stretching frequencies are higher by about 20−50 cm^{-1}, with correlated levels giving a greater change. The bending modes are hardly affected by the additional water. The sulfate modes correspond as follows: for C_{3v}, $A_1 \rightarrow A_1$, $E \rightarrow E$, $T_2 \rightarrow A_1 + E$; for C_2, $A_1 \rightarrow A$, $E \rightarrow 2A$, $T_2 \rightarrow A + 2B$. As compared to the dihydrate, these modes are slightly increased in frequency.

3.2.5. $SO_4^{2-}\cdot(H_2O)_4$. At this point, we note that the tetraaqua structures are complementary to the diaqua structures in the sense of the occupied/vacant water site reversal, and thus the same point groups should be encountered.

A fourth water may bind to sulfate to give two possible structures. A C_s structure may arise from coordination of a single water from any of the triaqua species previously discussed. The number of hydrogen bonds coordinated to each sulfate oxygen is then 3, 2, 2, and 1. A D_{2d} structure can only arise from the C_2 triaqua structure, with each oxygen possessing two hydrogen bonds. The D_{2d} structure is very slightly electronically favored by between 0.2 and 1.2 kJ/mol, depending on the level of theory. Differences between zero point and temperature corrections are less than 0.05 kJ/mol.

The metrical parameters of both species are given in Table S13. The trends are similar as those for the triaqua species. For comparable hydrogen bonds, those in the triaqua are slightly shorter and may indicate some cooperative effects.

The frequencies of all species are given in Tables S14 and S15. We note that MP2/6-31+G* frequencies could not be carried out here because of computational restrictions. Comparing the C_2 trihydrated sulfate with the D_{2d} tetrahydrated sulfate, the OH stretching frequencies are higher by about 30−40 cm^{-1}, with correlated levels giving a greater change. The bending modes are hardly affected by the additional water. The sulfate modes, in general, are very slightly increased in frequency.

3.2.6. $SO_4^{2-}\cdot(H_2O)_5$. The only structure has symmetry C_{2v}. The metrical parameters are given in Table S16. At the correlated levels the O···H distance is slightly longer between comparable hydrogen bonds in the pentaaqua as compared with the tetraaqua species. No correlated frequency calculations could be carried out for this structure. As compared to the tetraaqua D_{2d} structure, the symmetric OH stretching modes are increased by about 10 cm^{-1}, whereas the asymmetric modes are increased by about 30 cm^{-1}.

3.2.7. $SO_4^{2-}\cdot(H_2O)_6$. The only structure has symmetry T_d, and thus we return to the symmetry of the naked sulfate itself. All of the hydrogen-bonding indicator distances are longer than those in the pentaaqua structure. The OH stretching modes are increased by about 25 cm^{-1}, whereas the asymmetric modes are increased by less than 10 cm^{-1}.

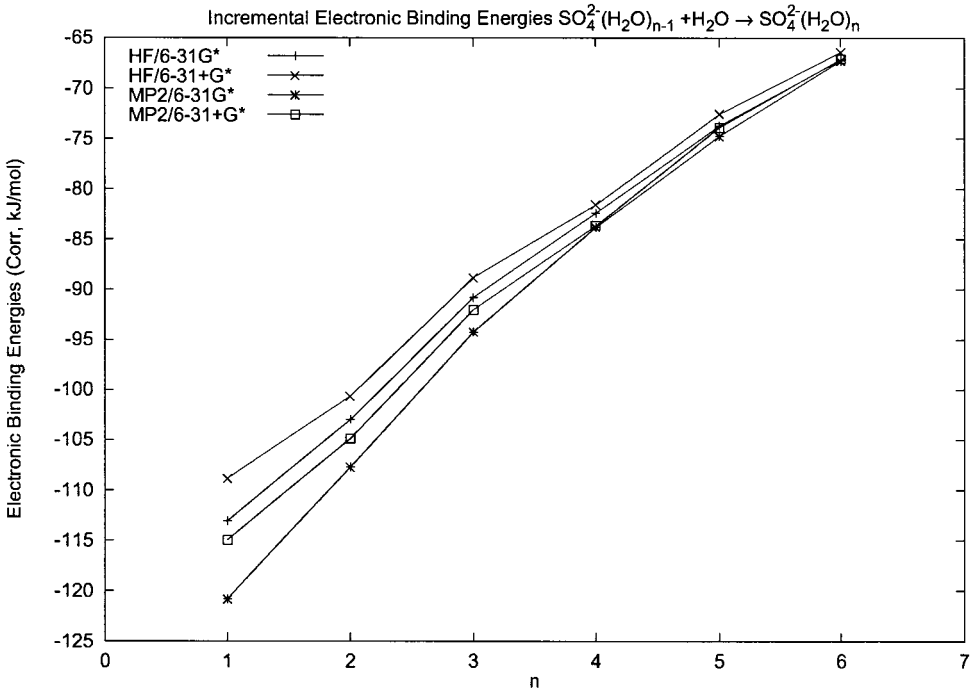

Figure 9. Sulfate incremental binding energies (corrected).

3.3. Discussion of Geometries. In Figure 3, we present the S−O distances in the sulfate ion itself as surrounded by various numbers of water molecules in various configurations. Although trends are not immediately apparent, if we distinguish the S−O distances by the number of hydrogen bonds formed to the oxygen, then we see that the data divides itself naturally by a series of parallel lines of positive slope. In general, the more hydrogen bonds to an oxygen of sulfate, the longer the S−O bond distance will become. However, adding waters to the cluster results in the shortening of all other S−O bonds in general, and so these two effects tend to cancel. Overall, the net effect is a shortening of the S−O distance between naked sulfate and the hexahydrated sulfate. The trends for the hydrogen-bonding indicators O···H (Figure 4), O···O (Figure 5), and S···O (Figure 6), are very clear: These distances lengthen as more waters hydrogen bond to the sulfate. This suggests that the hydrogen bonding becomes weaker as more waters bind to sulfate.

Experimental values of the O···O distance fall at about 2.88 Å.[30] Our MP2/6-31+G* distance for the hexaaqua cluster of 2.90 Å is slightly higher than this range, so the agreement is reasonable. However, experimental values of the S···O distance fall at about 3.79 Å, and our calculated value of 3.50 Å is much too short. We speculate that six waters in the first hydration shell of sulfate may not be enough to accurately describe the S···O distance, and that more waters are needed. These waters, if coordinated directly to the sulfate via hydrogen bonds, must begin to doubly occupy the six sites described before. We anticipate that this will result in the breaking of one of the two extant hydrogen bonds to the water already present at the same site and lengthen the S···O distance. Indeed, the structure found by Cannon[23] via MD simulation possesses this feature.

3.4. Discussion of Vibrational Frequencies. Figure 7 presents the vibrational frequencies of the clusters investigated at the HF/6-31+G* level. We note that, upon hydrating the sulfate ion with six waters, the frequencies increase by 20−30 cm^{-1}, with the exception of the $\upsilon_4(T_2)$ deformation mode, which undergoes only a very slight increase as more waters are added. The experimental values of the frequencies of sulfate in water (as the ammonium sulfate solution) are 452, 617, 981, and 1110 cm^{-1}. It is clear that the Hartree−Fock calculation of both the naked and the hexaaqua sulfate overestimates the vibrational frequency as compared to experiment, with the agreement getting worse as more waters are added! However, it is well-known that Hartree−Fock theory overestimates the frequencies and usually needs to be scaled to account for both deficiencies in theory and neglect of anharmonic contributions. For the naked ion, we derived scaling factors for frequencies by linear regression. The Hartree−Fock values for basis sets A−C are 0.933, 0.964, and 0.962 with standard errors of 0.012, 0.006, and 0.006. The corresponding MP2 values are 1.015, 1.088, and 1.073, with standard errors of 0.019, 0.008, and 0.004, respectively. Here, the combination of MP2 with a large basis set improves the agreement with the experiment but at much computational expense. For the hexahydrate, the HF/A and HF/B values are 0.929 and 0.942, with standard errors of 0.012 and 0.006. After scaling, the relative error with and without water is about the same.

The experimental fwhh of the sulfate bands are given in Table 1 as 34, 40, 6, and 80 cm^{-1}. Normally, to get properties of this type from ab initio calculation, one must perform molecular dynamics simulation (either Born−Oppenheimer or Car−Parinello). However, if we examine the splitting of degenerate modes in the mono through pentaaqua clusters and average these values, we obtain 9, 16, 0, and 51 cm^{-1}. If we consider just the pentahydrated species, we obtain 13, 13, 0, and 41 cm^{-1}. Taking the maximum values over all species, we obtain 23, 20, 0, and 80 cm^{-1}. We see that, for the case of degenerate modes, the prediction based upon the various splitting patterns qualitatively matches the experimentally observed bandwidth. Our interpretation of this interesting result is as follows. In solution, although the sulfate ion has effective T_d symmetry, at any given time, there may be water molecules entering and leaving the first hydration shell. Some of these instantaneous structures may look similar to the static structures calculated. The set of static structures calculated here could be regarded as a "sampling" of the sulfate environment. The concomitant reduction of symmetry destroys the degeneracy and the mode splits. When several of

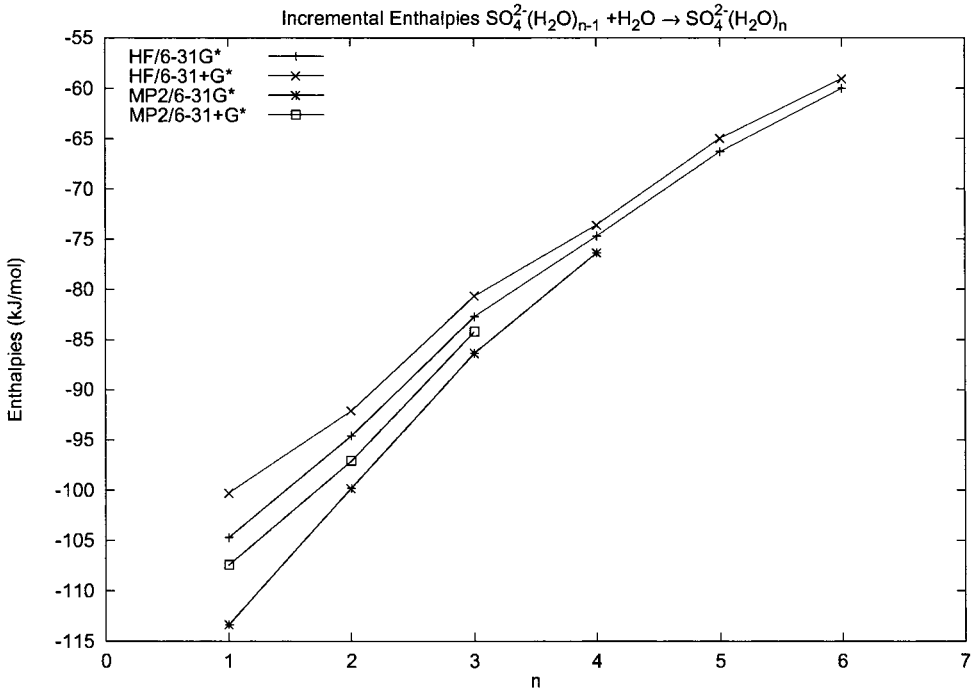

Figure 10. Sulfate incremental binding enthalpies.

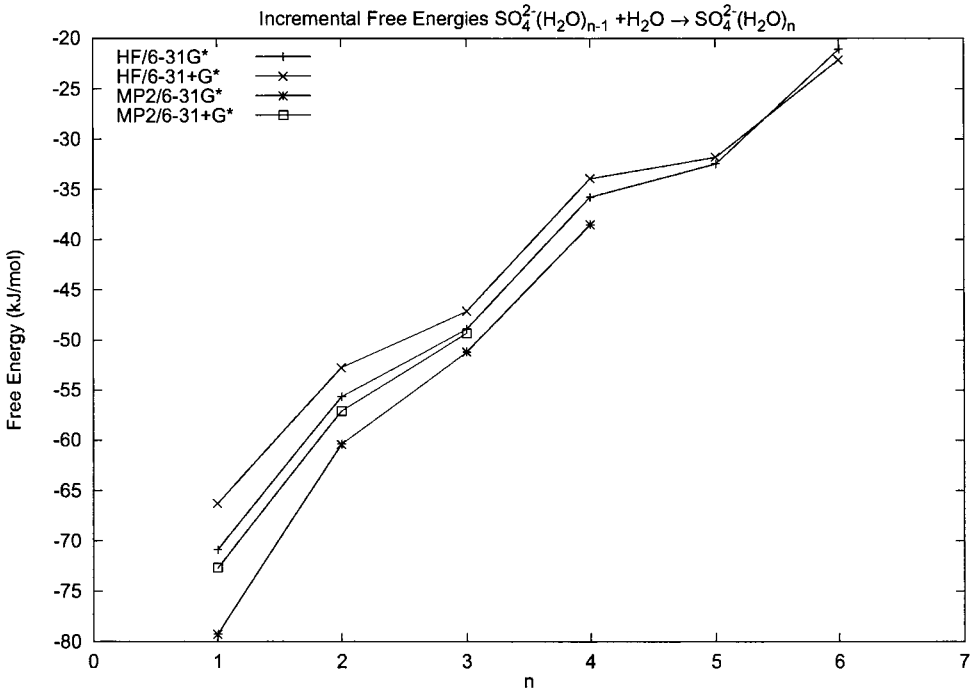

Figure 11. Sulfate incremental binding free energies.

these are averaged together, the result is an inhomogeneously broadened band of the "effective" T_d structure.

3.5. Discussion of Binding Energies. The incremental binding energies of sulfate with water, uncorrected for BSSE effects, are given in Figure 8. A comparison of the results for the 6-31G* and 6-31+G* basis sets indicate a large effect of the diffuse functions on the binding energy, with a larger effect at the correlated level. This suggests that the diffuse function is reducing the effect of BSSE and lowering the magnitude of the binding energy. This is indeed verified in the BSSE-corrected energies of Figure 9, in which the values are much more consistent across various levels, which suggests that the BSSE-free binding energy is not much affected by correlation energy. The BSSE content of the sulfate ion itself is reduced significantly by adding diffuse functions, whereas the BSSE content of the water remains unchanged. This may be ascribed to the fact that the HF/6-31+G* basis set does not contain diffuse functions on the water hydrogens. Because it is these atoms that are interacting with the sulfate, the BSSE content is hardly affected.

The addition of thermal corrections to give the binding enthalpies results in a slight stabilization of the larger clusters, as seen in Figure 10, whereas including the effects of entropy to give the binding free energies as in Figure 11 clearly destabilizes the larger clusters, although these are still negative.

4. Conclusions

The Raman spectrum of aqueous ammonium sulfate has been measured. A series of ab initio calculations at several levels of theory on several hydrated sulfate moieties has been carried out and structural, energetic, and vibrational characteristics have been determined. For the most part, the structural data as determined from experiment were reproduced by our calculations. The vibrational frequencies as obtained from solution Raman measurements were reproduced after suitable scaling of the theoretical results for the unsolvated and hexasolvated sulfates. Some insight into the experimentally observed line widths of the degenerate modes was obtained by carrying out an analysis of the unsymmetric structures of the partially solvated clusters.

Note Added in Proof. Very recently (Wang, X.-B.; Nicholas, J. B.; Wang, L.-S. *J. Chem. Phys.* **2000**, *113*, 10837−10840), sulfate ion − water clusters have been observed in the gas phase by electrospray mass spectrometry and photoelectron spectroscopy, and the interpretations supported by density functional calculations at the B3LYP/aug-cc-pVTZ//B3LYP/TZVP+ level. These results support our findings that the dianion is preferred in clusters with three or more waters.

Acknowledgment. The authors thank the Computing and Communications Department, Memorial University of Newfoundland, for computer time.

Supporting Information Available: Geometries, frequences, and total energies of sulfate ion structures (Tables S1−S20). This material is available free of charge via the Internet at http://pubs.acs.org.

References and Notes

(1) Richens, D. T. *The Chemistry of Aqua Ions*; Wiley: Chichester, 1997.

(2) Pye, C. C. *Int. J. Quantum Chem.* **2000**, *76*, 62−76.

(3) Pye, C. C.; Rudolph, W.; Poirier, R. A. *J. Phys. Chem.* **1996**, *100*, 601−605.

(4) Rudolph, W.; Brooker, M. H.; Pye, C. C. *J. Phys. Chem.* **1995**, *99*, 3793−3797.

(5) Rudolph, W. W.; Pye, C. C. *J. Phys. Chem. B* **1998**, *102*, 3564−3573.

(6) Pye, C. C.; Rudolph, W. W. *J. Phys. Chem. A* **1998**, *102*, 9933−9943.

(7) Rudolph, W. W.; Pye, C. C. *Phys. Chem.-Chem. Phys.* **1999**, *1*, 4583−4594.

(8) Rudolph, W. W.; Pye, C. C. *J. Phys. Chem. A* **2000**, *104*, 1627−1639.

(9) Rudolph, W. W.; Pye, C. C. *Phys. Chem.-Chem. Phys.* **2000**, *2*, 5030−5040.

(10) Rudolph, W. W.; Pye, C. C., manuscript in preparation.

(11) Rudolph, W. W.; Pye, C. C., unpublished results.

(12) Rudolph, W.; Schönherr, S. *Zeit. Phys. Chem.* **1991**, *172*, 31−48.

(13) Rudolph, W. W.; Brooker, M. H.; Tremaine, P. *Zeit. Phys. Chem.* **1999**, *209*, 181−207.

(14) Rudolph, W. W.; Brooker, M. H.; Tremaine, P. *J. Sol. Chem.* **1999**, *28*, 621−630.

(15) Rudolph, W. W.; Irmer, G. *J. Sol. Chem.* **1994**, *23*, 663−684.

(16) Rudolph, W. W. *J. Chem. Soc., Faraday Trans.* **1998**, *94*, 489−499.

(17) Rudolph, W.; Brooker, M. H.; Tremaine, P. *J. Sol. Chem.* **1997**, *26*, 757−777.

(18) Rull, F.; Balarew, C.; Alvarez, J. L.; Sobron, F.; Rodriguez, A. *J. Raman. Spectrosc.* **1994**, *25*, 933−941.

(19) Rull, F.; Sobron, F. *J. Raman. Spectrosc.* **1994**, *25*, 693−698.

(20) Rull, F.; Ohtaki, H. *Spectrochim. Acta A* **1997**, *53*, 643−653.

(21) Rull, F. *Z. Naturforsch. A* **1994**, *50*, 292−300.

(22) Martinez, A. Rodriguez; Grañón, F. Sobron; Pérez, F. Rull; Colorado, A. C. Prieto; Edwards, H. G. M. *Appl. Spectrosc.* **1995**, *49*, 1131−1136.

(23) Cannon, W. R.; Pettitt, B. M.; McCammon, J. A. *J. Phys. Chem.* **1994**, *98*, 6225−6230.

(24) Gaussian 92/DFT, Revision F.4, Frisch, M. J.; Trucks, G. W.; Schlegel, H. B.; Gill, P. M. W.; Johnson, B. G.; Wong, M. W.; Foresman, J. B.; Robb, M. A.; Head-Gordon, M.; Replogle, E. S.; Gomperts, R.; Andres, J. L.; Raghavachari, K.; Binkley, J. S.; Gonzalez, C.; Martin, R. L.; Fox, D. J.; Defrees, D. J.; Baker, J.; Stewart, J. J. P.; Pople, J. A. Gaussian, Inc.: Pittsburgh, PA, 1993.

(25) C-F 6-31G: Hehre, W. J.; Ditchfield, R.; Pople, J. A. *J. Chem. Phys.* **1972**, *56*, 2257−2261; H, C-F polarization functions: Hariharan, P. C.; Pople, J. A. *Theor. Chim. Acta (Berlin)* **1973**, *28*, 213−222; Li-B: Dill, J. D.; Pople, J. A.; *J. Chem. Phys.* **1975**, *62*, 2921−2923; Na-Ar: Francl, M. M.; Pietro, W. J.; Hehre, W. J.; Binkley, J. S.; Gordon, M. S.; Defrees, D. J.; Pople, J. A. *J. Chem. Phys.* **1982**, *77*, 3654−3665.

(26) H, Li-F diffuse: Clark, T.; Chandrasekhar, J.; Spitznagel, G. W.; v. R. Schleyer, P. *J. Comput. Chem.* **1983**, *4*, 294−301; Na-Cl diffuse: Frisch, M. J.; Pople, J. A.; Binkley, J. S. *J. Chem. Phys.* **1984**, *80*, 3265−3269.

(27) An anonymous referee (A) suggested that we try a full MP2 calculation with the 6-311++G** basis set. We report that the difference between full MP2 and frozen core MP2 structures using this basis set gave structures for the sulfate and its monohydrate with no significant difference in angles and bond lengths (<0.001 Å) except for the S···O distance, which differed by about 0.003 Å. The frequencies were identical to within 3 cm^{-1}.

(28) Fujita, K.; Kimura, M. *J. Raman Spectrosc.* **1981**, *11*, 108−111.

(29) We would like to thank an anonymous referee (B) for reminding us that a negative sign of the orbital energy is not a sufficient condition for proving the stability of a dianion, due to the use of a restricted Hartree−Fock wave function and subsequent perturbation treatments. We dealt with this problem in the following way. For each given stoichiometry, we selected the most stable doubly charged species. With the optimized geometry at each corresponding restricted level, we performed a single-point calculation on the singly charged radical anion using Gaussian 98 (Rev. A.9, Frisch, M. J. et al., Gaussian, Inc., Pittsburgh, PA 1998) at the unrestricted level, including spin projection for the MP2 calculations (as UHF/B, UMP2/B, and PMP2/B, and for the smallest two clusters, with basis set C). Initial guess orbitals were taken from the doubly charged ion because the default guess resulted in convergence to a different state of higher energy. Energy differences between the two versions of Gaussian for the dianion were less than 0.0001 au. The single point calculation should suffice because the SOMO is a nonbonding orbital. The results are given in Table S20. The resulting wave functions had moderate spin contamination (S^2 about 0.85 versus 0.75 expected for a doublet) which upon projection stabilized the structures by about 25 kJ/mol. The sulfate dianion is preferentially stabilized by water, in accord with a simple Born model for a more highly charged ion, but in the gas phase is unstable with respect to electron loss (by 90−150 kJ/mol). For the monohydrate, UHF theory predicts a strong preference for the singly charged ion (85 kJ/mol) whereas UMP2 theory predicts only a slight preference (7 kJ/mol). For the dihydrate, UHF predicts a strong preference for the dianion (51 kJ/mol), whereas UMP2 theory predicts only a slight preference (1 kJ/mol). The dianion is preferred for structures with more than two waters.

(30) Caminiti, R.; Paschina, G.; Pinna, G.; Magini, M. *Chem. Phys. Lett.* **1979**, *64*, 391−395.